Available online at www.sciencedirect.com
SCIENCE DIRECT®
Journal of Non-Crystalline Solids xxx (2006) xxx–xxx
JOURNAL OF NON-CRYSTALLINE SOLIDS
www.elsevier.com/locate/jnoncrysol

Stimulated structural transformations in $Se_{0.6}Te_{0.4}/SiO_x$ nano-layered composite

S. Kokenyesi [a,*], M. Malyovanik [b], V. Cheresnya [b], M. Shiplyak [b], A. Csik [a,1]

[a] University of Debrecen, Egyetem ter 1, 4010 Debrecen, Hungary
[b] Uzhgorod National University, Pidhirna 46, 88000 Uzhgorod, Ukraine

Abstract

The influence of nanostructuring on photo- and thermo-stimulated structural transformations and related changes of optical, thermodynamical and electrophysical parameters were investigated in $Se_{0.6}Te_{0.4}/SiO_x$ nano-multilayer structures and compared with the same changes in single amorphous $Se_{0.6}Te_{0.4}$ films. It was established that stimulated crystallization processes in an amorphous $Se_{0.6}Te_{0.4}$ model material that easily undergo stimulated crystallization depend on the presence of matrix in the nano-layered structure which enables additional operation of the optical recording in this type of chalcogenide materials for data storage.

PACS: 42.70.Gi; 42.70.Ln

Keywords: Conductivity; Vapor phase deposition; Chalcogenides; Nano-composites; Photoinduced effects

1. Introduction

Three main types of photo-induced structural transformations (PST) in amorphous chalcogenide semiconductor layers can be distinguished: (i) structural transformations within amorphous phase, (ii) photo-induced crystallization or amorphyzation, (iii) photo-induced mass transport. The first two types are widely investigated [1–4] while the third is usually connected with silver diffusion [5] or interdiffusion in Se/As_2S_3-type nano-multilayers [6,7] and is less investigated up to now. The photo-induced crystallization–amorphyzation processes are in the focus of research and development since they serve the basis for phase-change optical memory devices [4,8]. These processes are investigated in thin films, but the role of interfaces, heterostructure formation can be essential for the transformation process [9]. The importance of interfaces is multiplied in the nano-layered films, nano-composites, especially for the crystallization process, which has size- and interface-dependent parameters [10,11]. Exploiting the peculiarities of nanostructures related to the change of thermodynamical parameters, conductivity and optical properties in nano-sized objects, additional possibilities to improve the data recording process are expected.

Inserting the light-sensitive glass, for example, from the typical, easily crystallizing Se_xTe_{1-x} system, into the certain matrix and changing the dimensions of these glass-elements, as well as the type of matrix, new effects are expected: stimulation of the solid-state reactions, crystallization, the shift of optical absorption edge. For example, the crystallization kinetics in thin Ge–Sb–Te films sandwiched between transparent protective layers depends on the type of these layers [9]. The establishment of interconnections between the compositional modulation at nanoscale (~3–10 nm) in $Se_{0.6}Te_{0.4}$ containing nano-multilayers (NML) and the changes of the optical and electrical parameters as well as the possible improvement of optical recording process in comparison with homogeneous $Se_{0.6}Te_{0.4}$ films were the aim of the present work.

* Corresponding author. Tel.: +3652415222; fax: +3652315087.
E-mail address: kiki@tigris.unideb.hu (S. Kokenyesi).
[1] On leave from Institute of Nuclear Research, Hungarian Academy of Sciences (ATOMKI), P.O. Box 51, Debrecen H-4001, Hungary.

0022-3093/$ - see front matter © 2006 Elsevier B.V. All rights reserved.
doi:10.1016/j.jnoncrysol.2005.11.084

2. Experimentals

$Se_{0.6}Te_{0.4}$ composition can be considered as a rather good glass former [10,12] which promotes obtaining amorphous film, that in turn can be easily crystallized by heating or illumination. $Se_{0.6}Te_{0.4}$ glasses were synthesized from pure Se and Te components in sealed quartz ampoules and used for thin film and multilayer fabrication. First, the single 100–700 nm thick $Se_{0.6}Te_{0.4}$ and 100 nm thick SiO_x layers were thermally evaporated in vacuum onto the Corning glass or Si wafer substrata to graduate the technology process. Periodical multilayer structures were fabricated by the method of successive thermal evaporation of $Se_{0.6}Te_{0.4}$ and SiO_x materials from the separated sources in a time- and mass-transport controlled deposition cycles on the similar substrata. SiO_x was used as an optically transparent (in a visible spectral range) barrier material between 3 and 10 nm thick $Se_{0.6}Te_{0.4}$ layers. The total thickness of the $Se_{0.6}Te_{0.4}/SiO_x$ nano-multilayers (NML) was usually 100–200 nm with a near equal thickness of active $Se_{0.6}Te_{0.4}$ and barrier SiO_x sub-layers, so the composition modulation period Λ was in the 5–10 nm range. The modulation period and the quality of the NML were determined by low angle X-ray diffraction (XRD) method. At the smallest periods ($\Lambda = 5$–6 nm) the structure of the NML most likely approaches the layer-arranged $Se_{0.6}Te_{0.4}$ clusters separated by similar SiO_x layers.

Structural transformations stimulated by heating or illumination in such samples were investigated at normal ambient conditions by standard XRD method (Siemens, $Cu_{K\alpha}$, $\lambda = 1.54$ Å) and by optical transmission, absorption and reflection measurements. Optical parameters and DC electrical conductivity were measured in a special chamber also at different temperatures of 290–430 K range, in darkness or at He–Ne laser illumination ($\lambda =$ 0.63 μm, output capacity 25 mW) that can be further focused to achieve high intensity of illumination at the surface of the samples. The optical transmission change always was measured with a very low intensity beam to avoid additional stimulated changes. Electrical measurements were performed on samples with in-plain geometry of carbon electrodes, which were deposited in two parallel scratches. The scratches were as deep as the total thickness of the NML, so when filled up with carbon paste they served as contacts to all parallel $Se_{0.6}Te_{0.4}$ sub-layers. Surface transformations of the samples were investigated by optical microscopy and NT-MDT-type AFM.

3. Experimental results and discussion

The main results of our experiments consist in the demonstration of the influence of the inert (non-chalcogenide) matrix on the light- and thermo-induced crystallization of $Se_{0.6}Te_{0.4}$ in a layered nanocomposite. Since the high crystallization ability of homogeneous $Se_{0.6}Te_{0.4}$ glass is known [10], it is not surprising that the thin film, obtained during deposition from vapor onto the cold substratum and so initially amorphous, can be easily transformed to the crystalline state either by direct heating up to the softening temperature or by irradiation. XRD experiments directly confirm it for annealed samples (see Fig. 1) and for illuminated ones, although these experiments for illuminated samples were less spectacular because of the small size of the illuminated spot in comparison with the X-ray beam diameter.

Stimulated crystallization causes correlated changes in the optical and electrical parameters of $Se_{0.6}Te_{0.4}$ thin films and NMLs (Fig. 2). The electrical conductivity was measured in the in-plaine direction, so the results can be compared in a single layer and in the NML, since in the latter case the conductivity of the SiO_x matrix is negligible in comparison with the $Se_{0.6}Te_{0.4}$ sub-layers. The temperature dependence of the conductivity was exponential both before and after the annealing and the corresponding acti-

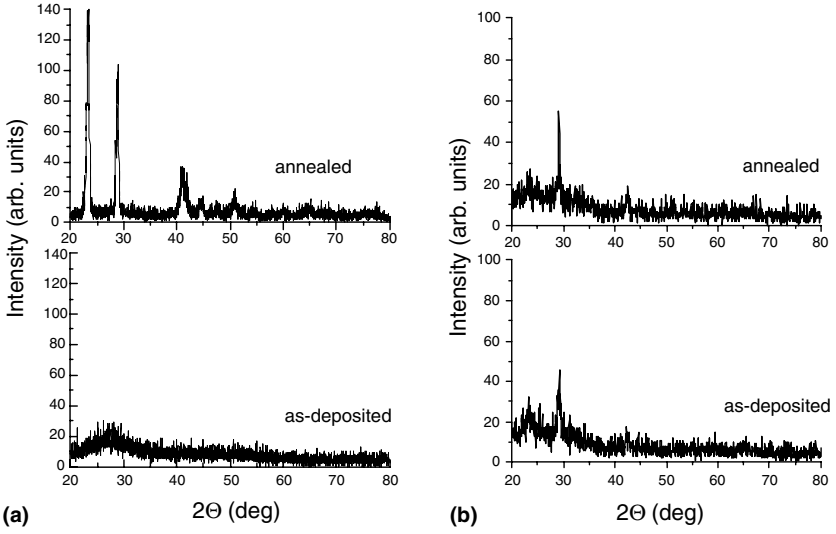

Fig. 1. X-ray diffraction picture for initial and annealed $Se_{0.6}Te_{0.4}$ films (a) and $Se_{0.6}Te_{0.4}/SiO_x$ nano-multilayers (NML) (b).

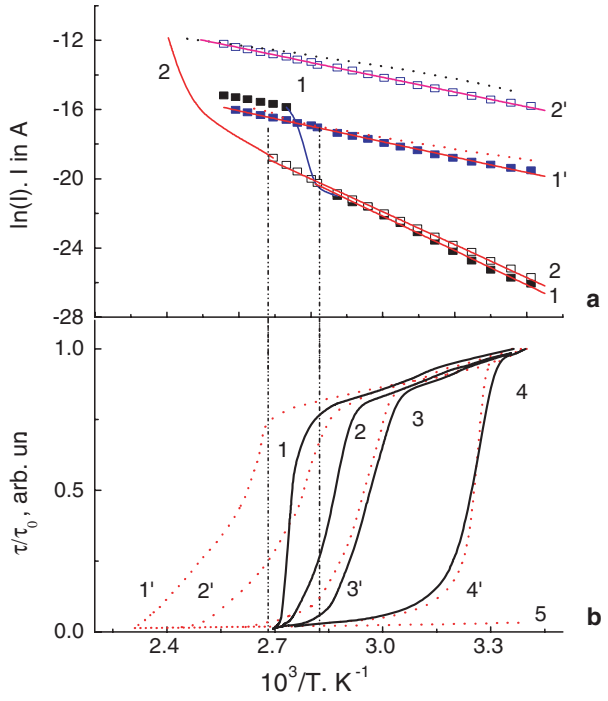

Fig. 2. (a) Temperature dependence of the DC conductivity current in $Se_{0.6}Te_{0.4}$ films before (1) and after (1′) annealing at 430 K, and the same for $Se_{0.6}Te_{0.4}/SiO_x$ MLS (2, 2′); (b) temperature dependence of the optical transmission τ relative to the initial τ_0 at $\lambda = 0.63$ μm for $Se_{0.6}Te_{0.4}$ (1–4), $Se_{0.6}Te_{0.4}/SiO_x$ (1′–4′). Curves (1–4) and (1′–4′) were measured under He–Ne laser illumination with intensities 0.1 W/cm^2, 3.5 W/cm^2, 7.0 W/cm^2 and 14 W/cm^2, correspondingly.

vation energies E_a were determined from the semi-logarithmic plot of current vs. temperature $\ln I = f(1/T)$ (see Fig. 2 and Table 1). The activation energies correspond to the half of the band gap of amorphous $Se_{0.6}Te_{0.4}$ and in the second cycle of the measurements, after the annealing, decrease to the E_a of the crystalline material.

The break points on the curves of temperature dependence of the electrical conductivity and optical transmission at 633 nm (Fig. 2(a) and (b)) correlate and both are shifted by 10–15 K to the higher temperatures in $Se_{0.6}Te_{0.4}/SiO_x$ nano-multilayers in comparison with a single layer. This fact can be explained by the simple influence of the interface conditions on the crystallization temperature in the NML, since the $Se_{0.6}Te_{0.4}$ do not wet the SiO_x surface. But the situation is more complex because the initial structure of the $Se_{0.6}Te_{0.4}$ film and NML is little different. Thin $Se_{0.6}Te_{0.4}$ film is initially amorphous while the NML contains crystalline nucleuses (Fig. 1(a) and (b)), so the stimulated crystallization processes start at different conditions and develop towards the total crystallization of $Se_{0.6}Te_{0.4}$, resulting in a little different structure of thin $Se_{0.6}Te_{0.4}$ films and $Se_{0.6}Te_{0.4}$ sublayers of NML (upper spectrums of annealed samples in Fig. 1(a) and (b)). As far as the XRD pikes for crystalline hexagonal Se and for Te are located very close (especially the pikes at $2\theta = 23.2$, 41.3) and only a pike near $2\theta = 29$ belongs to Se, not to Te, and all pikes are suppressed in the NML, it may be concluded that the resulting composition of crystallites are similar in both cases and that only their number and dimensions are different. The mechanism of this process can be explained taking into account the role of the illumination that essentially stimulates the crystallization.

Table 1
Activation energies for DC electrical conductivity

Material	E_a, eV (as deposited)	E_a, eV (annealed)
$Se_{0.6}Te_{0.4}$	0.85 ± 0.02	0.38 ± 0.02
$Se_{0.6}Te_{0.4}/SiO_x$	0.83 ± 0.02	0.37 ± 0.02

The increase of the illumination intensity P causes a low-temperature shift of the crystallization threshold and a simultaneous change of the shape and slope of the temperature dependence of optical transmission τ relative to the initial one τ_0 at $\lambda = 633$ nm (Fig. 2(b)). The calculated according to [13] maximum increase of the temperature in the layer caused by focused laser beam in our case was not more than 8–12 K. At the same time the crystallization threshold decreases to 30–50 K (see Fig. 2(b)). The dominant role of the light and not of the temperature change in the crystallization process was also supported by low-temperature (190 K) measurements of τ/τ_0, which were not essentially changed in comparison with τ/τ_0 measured at 293 K. At the maximum illumination intensity $P =$ 14 W/cm^2 the shape of the curves 4, 4′ in Fig. 2 is almost identical, which supports the similarity of the light stimulated crystallization process in $Se_{0.6}Te_{0.4}$ and in the NML at these conditions. At low illumination intensities the shape of the curves 1, 1′ in Fig. 2 reveals that in the single $Se_{0.6}Te_{0.4}$ layer the light induced nucleation process prevail in the whole volume, while in the NML the prevailing process is the crystallite growth, because the nucleuses exist in the as-deposited NML (Fig. 1). These nucleuses in the amorphous $Se_{0.6}Te_{0.4}$ are well separated, the conductivity is under the percolation threshold and is characterized by the same temperature dependences (curves 1, 2 in Fig. 2(a)). After the heating up to 350–380 K (or proper illumination) crystallization occurs and the DC conductivity changes similarly in successive cycles of heating (curves 1′, 2′ in Fig. 2(a)) or cooling (dotted curves in the same figure). The transformation is irreversible, since during the successive cooling the optical transmission does not restore (see the almost horizontal curve 5 in Fig. 2(b)).

The details of the photo- and thermo-induced crystallization process were analyzed in the framework of Avrami–Kolmogorov model [14]. The fraction x of the crystallized layer, measured by the change in the optical density of the layer at 633 nm, may be written as

$$x = 1 - \exp(-V_{ex}), \quad (1)$$

where $V_{ex} = \pi d N v^n t^n$ and v is the one-dimensional growth rate; n is the reaction order; N is the number of nucleation sites and d, the film thickness.

The growth rate can quite often be represented in Arrhenius form $v = v_0 \exp(-E_a/kT)$, where E_a is the activation energy; v_0, a constant and k, the Boltzmann constant. Then

$$V_{ex} = \pi d N v_0^n \exp(-nE_a/kT)t^n \quad (2)$$

and

$$x = 1 - \exp(-\pi d N v_0^n \exp(-nE_a/kT)t^n) = 1 - \exp(-Kt^n), \quad (3)$$

where $K = K_0 \exp(-nE_a/kT)$ is the growth constant and t is the time required to reach the x state.

So the E_a can be determined and used together with n for the definition of the transformation process.The reaction order n depends in a complex and ambiquous way on the nucleation and crystal growth, especially in a complex heterogeneous material, but in general it is expected that crystal grain growth dominates the process if n is in the range 1.0–1.3, and $n \geqslant 1.5$ if a grain growth occurs with nucleation. For $1.5 \leqslant n < 2.5$ the decrease of the nucleation rate with a progress of the grain growth is expected in Ge–Sb–Te amorphous thin layers sandwiched between dielectric layers [9].

Since the following dependence can be written as

$$\ln(-\ln(1-x)) = \ln(\pi d N v_0^n) - nE_a/kT + n \ln t, \quad (4)$$

n may be determined from the dependence $\ln(-\ln(1-x)) = f(\ln t)$ (Fig. 3), as well as the activation energy E_a from the dependence $\ln(-\ln(1-x)) = f(1/T)$.

The results presented in Fig. 3 and Table 2 testify the prevailing role of the nucleation processes ($1.5 < n < 2.5$) at low intensity irradiation and high temperatures in $Se_{0.6}Te_{0.4}$ (Fig. 3, 1″). When the P increases two effects are observable: nucleation and crystal growth ($n < 1.5$). What is more, crystallites are formed in the whole volume of the layer, not from the surface towards the substratum, which is supported by the slope of the increase of the optical reflection during the illumination. At the same time in $Se_{0.6}Te_{0.4}/SiO_x$ nano-layered composite the crystallites, which were present in the as-deposited structure, start to grow in the whole volume under the influence of the heating even without illumination (Fig. 3, curve 2′). Laser illumination stimulates additional nucleation and the growth of the crystallites as well (Fig. 3, curves 2, 2′).

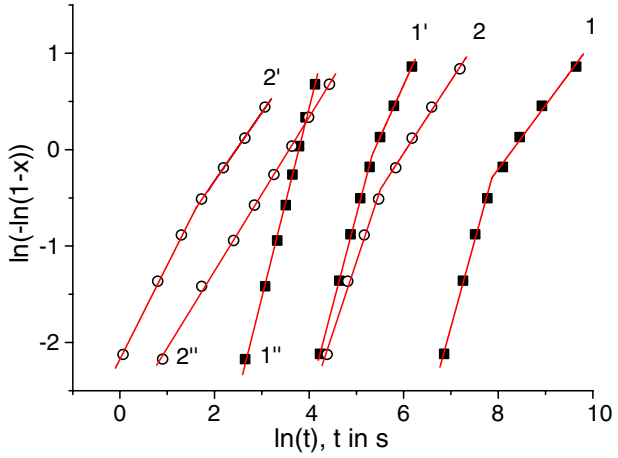

Fig. 3. Plot of $\ln[-\ln(1-x)]$ vs $\ln(t)$ at temperature $T = 293$ K and power density of the laser illumination $P = 28$ W/cm^2 for $Se_{0.6}Te_{0.4}$ (1), $Se_{0.6}Te_{0.4}/SiO_x$ (2), as well as at $T = 343$ K and $P = 28$ W/cm^2 for $Se_{0.6}Te_{0.4}$ (1′), $Se_{0.6}Te_{0.4}/SiO_x$ (2′) and at $T = 373$ K, $P = 0.1$ W/cm^2 for $Se_{0.6}Te_{0.4}$ (1″), $Se_{0.6}Te_{0.4}/SiO_x$ (2″).

Table 2
Rate orders of the crystallization processes

Material	n at $T = 293$ K, $P = 28$ W/cm^2	n at $T = 343$ K, $P = 28$ W/cm^2	n at $T = 373$ K, $P = 0.01$ W/cm^2
$Se_{0.6}Te_{0.4}$	1.79 ± 0.07 0.66 ± 0.05	1.86 ± 0.03 1.08 ± 0.01	1.96 ± 0.03
$Se_{0.6}Te_{0.4}/SiO_x$	1.50 ± 0.08 0.75 ± 0.03	0.97 ± 0.03 0.71 ± 0.05	0.78 ± 0.04

Our experimental data, presented in Table 2 refer to the more dominant role of the crystalline grain growth and enhanced transformations rates in $Se_{0.6}Te_{0.4}/SiO_x$ NMLs in comparison with single $Se_{0.6}Te_{0.4}$ layer. It is not surprising due to the definite presence of crystalline nucleuses or even crystallites in as deposited NMLs (Fig. 1(b)), which in turn may be explained by the influence of heterogeneous nucleation at interfaces in the as-prepared NMLs as well as at the stage of MLS deposition, which includes a rather low-temperature evaporation of $Se_{0.6}Te_{0.4}$ (~640 K) and a high-temperature evaporation of SiO_x component (~1000 K). The shape of the curve 1 in Fig. 2(b) corresponds to the grain growth with nucleation in a single $Se_{0.6}Te_{0.4}$ layer. Under increasing illumination intensity the character of such curves in $Se_{0.6}Te_{0.4}$ become very similar to the curves 3′, 4′ for $Se_{0.6}Te_{0.4}/SiO_x$ NML, which indicates the increasing role of the additional fast nucleation and growth at the initial stage of the transformation up to the saturation of nucleus concentration and the following slower crystal grain growth. In spite of the presence of nucleuses in as-prepared $Se_{0.6}Te_{0.4}/SiO_x$ such MLS is thermally more stable in comparison to a single layer (curves 2 in Fig. 2(a) and 1′ in Fig. 2(b)), which can be explained by the presence of additional stresses and size restrictions, which influence phase change temperatures in nanostructures [14], and also by the surface reactivity and chemical affinity of the combined layers [9].

The role of the illumination consists first of all in the essential lowering of the activation energies of the structural transformations (see Table 3), i.e. stimulation of this process even without heating, which is characteristic for amorphous chalcogenides [1–4], especially due to the so called photoplasticity and enhanced mobility of the structural elements under illumination [15].

So, making the initial state of MLS more stable with respect to the temperature in comparison with a single layer, we can get more fast switch at high illumination

Table 3
Activation energies E_a and growth constants K for thermo- and photo-stimulated crystallization

Material	K, s^{-1} (at $T = 293$ K)	K, s^{-1} (at $T = 343$ K)	E_{ac}, eV (thermo)	E_{ac}, eV (photo)
$Se_{0.6}Te_{0.4}$	$(1.1 \pm 0.1) \times 10^{-4}$	$(4.1 \pm 0.2) \times 10^{-3}$	1.0 ± 0.1	0.7 ± 0.1
$Se_{0.6}Te_{0.4}/SiO_x$	$(9.7 \pm 0.1) \times 10^{-4}$	$(3.5 \pm 0.2) \times 10^{-2}$	1.2 ± 0.1	0.6 ± 0.1

intensities in a steady state process. This effect may be used for the development of thin nano-multilayer phase-change memory element, which can be read-out either optically or electrically. It will be interesting to see the backward process of amorphization, but it needs special pulsed illumination and will be performed later on together with a pulsed recording process. The present results support the possibility of efficient operation of the recording efficiency by nano-structurization of the chalcogenide-based recording material.

4. Conclusions

Photo- and thermo-stimulated crystallization of nanometer-thick $Se_{0.6}Te_{0.4}$ films embedded into SiO_x matrix in the form of nano-multilayer structure can be investigated by the comparative measurements of optical transmission and electrical conductivity change. It was found that the as-prepared $Se_{0.6}Te_{0.4}/SiO_x$ nano-structure contains crystallites which to a considerable extent determines the transformation due to the grain growth limited process. Illumination essentially enhances crystallization both in the single $Se_{0.6}Te_{0.4}$ layer and in the $Se_{0.6}Te_{0.4}/SiO_x$ structure, making the process more nucleation-dependent and fast which results in the higher efficiency of the stimulated transformation and optical recording in such a nano-layered structure.

Acknowledgements

This work was supported by Ukrainian–Hungarian R&D co-operation Grant UKR-19/2004 and Hungarian OTKA Grants # T046757 and D048594.

References

[1] J. Singh, K. Shimakawa, Advances in Amorphous Semiconductors, CRC Press, 2003.
[2] H. Jain, J. Optoelectron. Adv. Mater. 5 (2003) 5.
[3] K. Shimakawa, A. Kolobov, S.R. Elliott, Adv. Phys. 44 (1995) 475.
[4] A. Kikineshi, in: Physics and Technology of Thin Films, IWTF 2003, World Scientific Publishing, Singapore, 2004, p. 318.
[5] I.Z. Indutnij, M.T. Kostishin, P.F. Romanenko, A.V. Stronskij, Infrared Res. Mater. 19 (1991) 239.
[6] M. Malyovanik, I. Ivan, A. Csik, G. Langer, D.L. Beke, S. Kokenyesi, J. Appl. Phys. 93 (2003) 139.
[7] V. Palyok, I.A. Szabo, D.L. Beke, A. Kikineshi, Appl. Phys. A 68 (1999) 489.
[8] M. Wuttig, Nature Mater. 4 (2005) 265.
[9] Norikazu Ohshima, J. Appl. Phys. 79 (1996) 8357.
[10] A. Feltz, Amorphe und Glasartige Anorganische Festkorper, Akademie, Berlin, 1983.
[11] M.I. Komnik, Size Effects in Thin Metallic Films, Moscow State University, 1986 (in Russian).
[12] V.B. Brasil, E. Mayer, J. Non-Cryst. Solids 348 (2004) 7.
[13] J. Burke, The Kinetics of Phase Transformations in Metals and Alloys, Pergamon, Oxford, 1965.
[14] E. Abraham, J.M. Halley, Appl. Phys. A 42 (1987) 279.
[15] M.L. Trunov, J. Non-Cryst. Solids 192&193 (1995) 431.